Li, Daming; Deng, Lianbing; Su, Qinglang; Song, Yong-Hua

Article

Providing a guaranteed power for the BTS in telecom tower based on improved balanced owl search algorithm

Energy Reports

Provided in Cooperation with:
Elsevier

Suggested Citation: Li, Daming; Deng, Lianbing; Su, Qinglang; Song, Yong-Hua (2020) : Providing a guaranteed power for the BTS in telecom tower based on improved balanced owl search algorithm, Energy Reports, ISSN 2352-4847, Elsevier, Amsterdam, Vol. 6, pp. 297-307, https://doi.org/10.1016/j.egyr.2020.01.006

Energy Reports 6 (2020) 297–307

Contents lists available at ScienceDirect

Energy Reports

journal homepage: www.elsevier.com/locate/egyr

Research paper

Providing a guaranteed power for the BTS in telecom tower based on improved balanced owl search algorithm

Daming Li [a,b,c], Lianbing Deng [a,b,d,*], Qinglang Su [c], Yonghua Song [e]

[a] The Post-Doctoral Research Center of Zhuhai Da Hengqin Science and Technology Development Co., Ltd, Guangdong Hengqin New Area, 519031, China
[b] Guangdong Qinzhi Science and Technology Research Institute, Guangdong Hengqin New Area, 519031, China
[c] Institute of Data Science, City University of Macau, Macau, 999078, China
[d] Huazhong University of Science and Technology, Hubei Wuhan, 430074, China
[e] Macao University, Macau, 999078, China

ARTICLE INFO

Article history:
Received 13 October 2019
Received in revised form 27 November 2019
Accepted 21 January 2020
Available online xxxx

Keywords:
Telecom tower
PEMFC
Owl search algorithm
Improved
Boost converter
DC distribution
Voltage regulation

ABSTRACT

The telecommunication industry is the technology of communication among humankind. One problem for this industry is to provide the required energy for its towers in the remote rural areas in the absence of the grid. This objection causes dependency of this industry to the diesel generators and battery banks as backup resources. Despite not being resilient and the effect of environment for the power supplies in diesel generators is still widespread. This paper presents a new optimized and environmentalist power supply configuration for the telecommunication tower based on the proton exchange membrane fuel cell (PEMFC). An optimized PI-based converter is also utilized to keep the source value reliable. For achieving optimized results for the PI controller, a developed version of the owl search algorithm is proposed. Simulation results have been applied in different conditions and the results are compared with Ziegler–Nichols, particle swarm optimization algorithm, and emperor penguins optimizer based PI controller to show the excellence of the proposed method.

1. Introduction

The world of telecommunication and information production is rapidly changing, and today we are witnessing their convergence with each other so that data and information are quickly and unimaginably transmitted to users around the world (Choi et al., 2019). It has undoubtedly led to widespread developments in all the social and economic spheres of humanity and its impact on human societies in a way that today's world is rapidly becoming a society based on telecommunication. The scope of its use and impact on different aspects of today's and future life of human societies has become one of the most important topics in the world today and has attracted the attention of many countries around the world (Mahajan et al., 2019). A significant issue which is recently mentioned in the telecommunication industry is the supply problem for the base transceiver station (BTS) of telecommunication tower, especially for the distant rural zones. BTS is a set of wireless and wired telecommunications equipment that facilitates communication between a mobile user and a public network. BTS stations are the most important component of GSM mobile networks. The antennas installed on these towers are connected to the network via microwave radio waves, trying to get a city-like area under the full coverage of a mobile network. Hence, providing a robust and non-stop power supply guarantees customer service quality (Kaur et al., 2017). In distant areas, guaranteed power supplying for BTSs is not an easy task, especially due to the unavailability of the national grid in this area.

Finding a reliable and economical solution to supply the BTS power installed in rural areas and away from the grid has become a challenge for mobile operators. Therefore, reviewing the available options for the BTS power supply in the telecommunications industry is crucial. One of the best appropriate selections for supplying a non-stoppable power for the distant areas is to use diesel generators (DG) (Ojo et al., 2019). A DG is a small power plant that usually takes on the task of generating electricity during an emergency that cuts off power for any reason. It can also as a fixed generator for the distant areas. A significant shortcoming of the DGs is that they have a high startup failure which is about 15%. To solve this problem, a battery bank can be employed (Paudel and Wasti, 2018). Since the environmental hazard impact of DGs, organizations are working on upgrading these power supplies collection based on green technologies like renewable technologies. Recently, the use of renewable energy technology such as wind systems, fuel cells, and photovoltaic has

* Corresponding author at: Guangdong Qinzhi Science and Technology Research Institute, Guangdong Hengqin New Area, 519031, China.
E-mail address: denglb@csu.edu.cn (L. Deng).

https://doi.org/10.1016/j.egyr.2020.01.006

been increased dramatically due to their easy access, the unending and the non-pollution of these sources to supply electricity to off-grid areas.

This makes the application of renewable energy resources important in the telecommunication industry (Hallur and Sane, 2018) such that the application of renewable energy resources like photovoltaic energy conversion systems and wind energy has been developed as the backup power supplies of the DGs (Aghajani and Ghadimi, 2018; Liu et al., 2017; Gollou and Ghadimi, 2017). In recent years, among different types of renewable resources, fuel cells are turning into one of the more interesting technologies for the long term backup for the telecommunication industry (Mirzapour et al., 2019). This is due to the fuel cell's characteristics such as higher efficiency for conversion, longer runtime (greater than 8 h), quiet operation, lower pollutant to the environment, low cost of maintenance, and rooftop installation capability.

There are plenty of research works about this category. For instance, Hosseini Firouz and Ghadimi (2016) introduced a robust configuration for a power system including the fuel cell as backup supply in the telecommunication applications. The method was testified in the practical position in a station with GSM and the results give 98.5% robustness for the fuel cell system during 260 cycles. Hamian et al. (2018) analyzed the effects of fuel cell technology along with photovoltaic system for a distant rural telecom system in Bangladesh. Proton exchange membrane fuel cell (PEMFC) is used as a popular type of fuel cell and then it connected to an upgraded photovoltaic system (solar). The paper claimed that the performance of the PEMFC was increased to 57.26%. The lifetime of the fuel cell was also analyzed.

Kaur et al. (2017) proposed another method based on proton exchange membrane fuel cells for using in the telecom supply system. The method used a simple closed-loop and genetic algorithm for intelligent interfacing unit that contains power electronic boost converter for power conditioning. The method guaranteed the tight voltage adjustment at the DC distribution bus of the base transceiver station. The method is simulated in MATLAB/Simulink platform and verified theoretically. The results give successful achievements that showed the feasibility of the presented system for robust operation of the telecom towers.

Leng et al. (2018) proposed an on-site hydrogen generation for BTS application for the fuel cell. They used two case studies for the analysis of the proposed system and the results showed that the hydrogen can improve the economics of power supply. Mirzapour et al. (2019) proposed a comparative analysis for power sources of the BTS. The main purpose of the method is to compare the feasibility of adopting renewable power sources for minimizing carbon emission, reducing the dependency on fossil fuel, and minimizing the cost of the system. A new model is presented to combine the sources with backup of diesel generator.

Akbary et al. (2019) modeled a hybrid system for powering remote BTS. The study's purpose was about providing a renewable energy source for supplying a remote BTS station. A hybrid renewable energy plant including a wind turbine, photovoltaic panels, and a fuel cell was provided. HOMER software was utilized for simulating the system. The final results showed that using renewable energy sources is feasible solutions to reduce the air contaminants and pollutants generated by sources such as diesel generators.

As it is clear from the literature, using renewable energies for the BTS is exponentially increasing and this is due to its advantages that were discussed before (Ebrahimian et al., 2018). Another case is that in most of these works, PEMFC is used as a popular fuel cell (Khodaei et al., 2018). This is due to its need to lower operating temperature which makes fewer need to thermal stress on components and warming up time (Bagal et al., 2018). Plus, due to the absence of mechanical parts like rotating parts in PEMFCs, they have not mechanical wear which makes them more reliable.

PEMFCs require hydrogen for feeding; this can be supplied by the bio-fuels or gas. This can be supplied by the nearby gas pipelines. For feeding the PEMFC, hydrogen is made by electrolyzing operation powered by different resources (Gheydi et al., 2016). From the literature, it can be concluded that the combination of the PEMFC with the BTS in the telecom tower can guarantee an adjustable energy resource for the BTS distribution bus in different operations. The voltage of PEMFC can be changed by oscillations in the voltage and temperature. This makes unreliable results for supplying the BTS station as a backup system.

In this study, a new optimized boost converter interfacing unit is proposed for covering this drawback. A boost converter is a component that levels up the voltage to a considered voltage level in DC bus. The research provides a new modified optimization algorithm, called Improved Owl search algorithm, for optimal control of the boost component for different reasons such as providing a fast response for the dynamic of the interfacing unit, adjusting the DC distribution voltage, and guaranteeing the reliability of the system under output oscillations of the PEMFC during load variation of telecom tower. Generally, The novelty and contributions of propose paper is summarized as follow:

- Proposing a new optimization algorithm for optimizing the PI controller on the boost converter.
- Improving the convergence and exploration shortcomings of the Owl Search Algorithm based on Chaos theory and LV mechanism.
- Proposing a new clean configuration based on the PEMFC for the Telecom.
- Analyzing the proposed optimized method based on different voltage and load fluctuating.

2. The architecture of the supply system for the BTS station

Fig. 1 shows the main configuration of a BTS station for the telecom tower. As it is observed, the BTS distribution system uses 48 V DC based on the high DC voltage of the system and its security. The component POL (point of loads) converter is adopted for providing the load end electronic equipment energy through the DC distribution bus.

Switch Mode Power Converter (SMPC) is used here as an electronic power supply to incorporate a switching regulator to convert electrical power efficiently in the distribution bus of the base transceiver station. Indeed, the reason for using SMPC in the system is to provide a filter for the input source and the telecom load oscillations to obtain a compressed adjusted voltage at the DC bus. This is because of the sensitivity of the telecommunication load to the voltage oscillations.

In the following, the main architecture of the BTS feeding system for the present study has been represented. To make a reliable system based on the explanations in the introduction, a 2.5 kW PEMFC is utilized as a clean energy resource to supply the BTS energy by receiving the oxygen and the hydrogen from a side to electricity generation based on chemical reaction and forms water vapor as a by-product. Fig. 2 shows this architecture. A significant profit of the PEMFC is that it does not require continuous maintenance checking.

As aforementioned, the output voltage of a PEMFC depends on variety of cases from load variations to an environmental condition like atmospheric pressure, humidity, and temperature which is changed between 15% to 30% below or above the output voltage and uses the other parts to keep the outpour voltage in 48

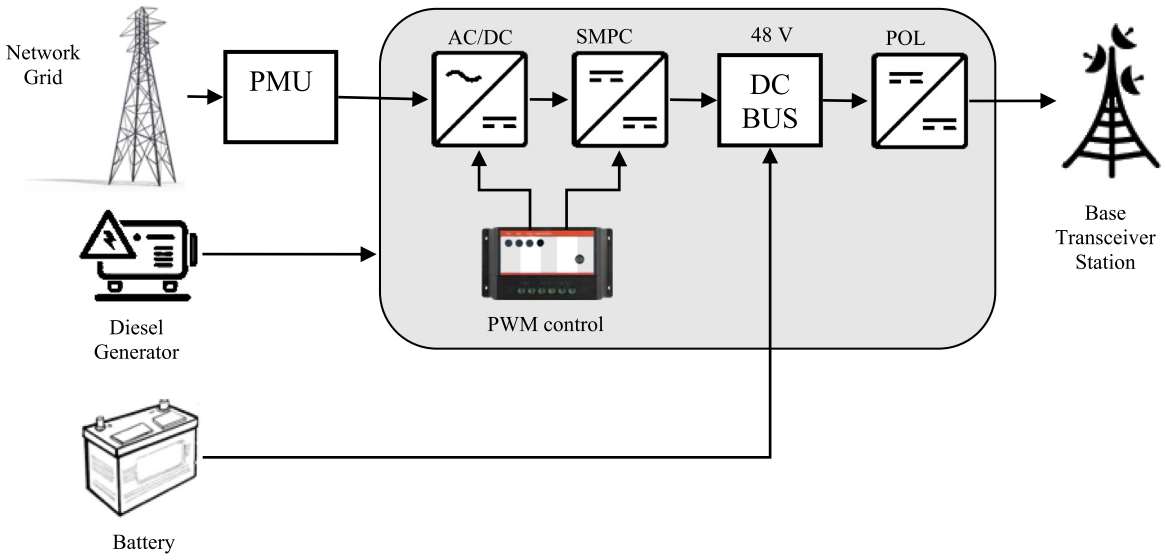

Fig. 1. The main configuration of a BTS station for the telecom tower.

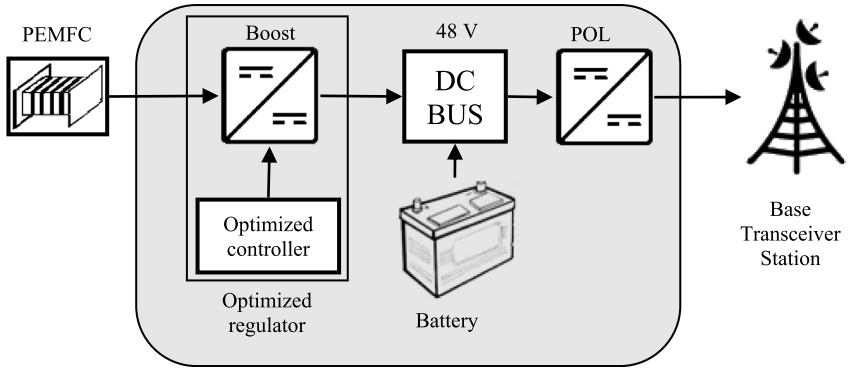

Fig. 2. The architecture of the proposed optimized BTS feeding system based on PEMFC.

Table 1
The required power for the telecom tower location in different BTS architectures (Kaur et al., 2017).

Architecture	Load		Total power (kW)
	DC (kW)	AC (kW)	
2 × 2 × 2	1.24	1.8	3.04
4 × 4 × 4	2.04	2.4	4.44
6 × 6 × 6	2.82	3.6	6.42

V at the DC bus. Table 1 illustrates the total power requirement of the telecom tower system for different BTS structures

In this study, the DC/DC boost converter in the regulator has been optimized based on a new technique to adjust the output voltage of the converter. The main purpose of the proposed optimized regulator is to keep the voltage of the PEMFC output voltage in the 48 V for the BTS distribution bus. The proposed regulator gives also a high-speed response that increases the speed of the total system.

3. Mathematical model of a fuel cell

Generally, PEMFCs are one of the most important sources of clean energy in the coming years. On the other hand, the possibility of producing hydrogen from renewable energy sources has doubled its attention in recent years. Fuel cells are simple to operate, with hydrogen and air (or oxygen) as reactants in the catalytic layer of the polymer membrane, producing electricity and water. It also provides sensors with the capability of generating power in the range of several watts to several megawatts, for use in a variety of applications, including propulsion for ships and trains to power generation. A PEMFC is a converter to turn the chemical reaction between oxygen and hydrogen into electrical energy and water. To model this component based on thermodynamic principles, the energy available across the cells is achieved as follows (Firouz and Ghadimi, 2016):

$$E_a = 1.23 - 8.5 \times 10^{-3} \times \left(\theta_{fc} - 298.15\right) + 4.31 \times 10^{-5} \times T \times ln\left(p_{H_2}\sqrt{p_{O_2}}\right) \quad (1)$$

where, θ_{fc} represents the fuel cell temperature (Kelvin) and the partial pressure of the oxygen and the hydrogen are as follows:

$$p_{O_2} = 0.5 \times RH_a \times p^{st}_{H_2O} \times \left(\frac{1}{\frac{RH_a \times p^{st}_{H_2O}}{p_a} exp\left(\frac{1.6 \times (i/A)}{\theta^{1.3}}\right)} - 1 \right) \quad (2)$$

$$p_{H_2} = 0.5 \times RH_a \times p^{st}_{H_2O} \times \left(\frac{1}{\frac{RH_c \times p^{st}_{H_2O}}{p_c} exp\left(\frac{4.2 \times (i/A)}{\theta^{1.3}}\right)} - 1 \right) \quad (3)$$

And the saturation pressure of the water vapor can be achieved by the following equation:

$$\log_{10}\left(p^{st}_{H_2O}\right) = -2.2 + 0.03 \times \left(\theta_{fc} - 273.15\right) - 0.92 \times 10^{-4}$$

$$\times \left(\theta_{fc} - 273.15\right)^2 + 0.14 \times 10^{-6} \times \left(\theta_{fc} - 273.15\right)^3 \quad (4)$$

And the output voltage for the cells is obtained based on the following formulation:

$$V_{cell} = E_a - \eta_{ma} - \eta_{al} - \eta_O \quad (5)$$

This means that the output voltage is received after subtracting the energy available from the internal losses inside the fuel cell, including mass transfer loss, ohmic loss, and activation loss.
where, the activation loss is achieved as follows:

$$\eta_{al} = -\left[\Psi_1 + \Psi_2\theta_{\mathrm{fc}} + \Psi_3\theta_{\mathrm{fc}} \ln\left(\frac{p_{O_2}}{5.1 \times 10^6 \times \exp\left(-498/\theta\right)}\right) + \Psi_4\theta_{\mathrm{fc}} \ln(\mathrm{i})\right] \quad (6)$$

Since the presence of the electrical resistance in electrodes and polymer membrane, Ohmic losses are also made by the following equation:

$$\eta_O = \left[R_c + \left(\frac{181.6\left(1 + 0.062 \times \left(\frac{\theta_{fc}}{303}\right) \times \left(\frac{i}{A}\right)^{2.5} + 0.03 \times \left(\frac{i}{A}\right)\right)}{A \times \left(\lambda - 3 \times \left(\frac{i}{A}\right) - 0.63\right) + A \times exp\left(4.2 \times \left[\frac{\theta_{fc} - 303}{\theta_{fc}}\right]\right)}\right)^{l}\right] \times i \quad (7)$$

Finally, the mass transfer loss is obtained by the following equation:

$$\eta_{ma} = -\beta \times ln\left(1 - \frac{i_{den}}{i_{limit,den}}\right) \quad (8)$$

In the above cases, $\Psi_1, \Psi_2, \Psi_3, \Psi_4, \mathrm{R_c}$ are obtained by the optimization methods as described in Eslami et al. (2019).

4. Mathematical modeling and optimizing the boost converter

Boost switching converter is a converter that increases the input voltage level to the output while reducing the current level. The booster converter is a class of switching power supplies and typically comprises two semiconductors (one diode and one transistor) and at least one stator element (inductor or capacitor or a combination of both). To reduce the ripple voltage, capacitor filters (sometimes combined with inductors) are added to the outputs and the inputs of these switching converters.

The boost power converter can be connected to any DC source such as fuel cell, battery, solar panel, rectifier, and DC generator. The process of converting a DC voltage to another DC voltage at a different level is called DC/DC conversion. As the converter switched on, the source of the voltage and the inductor form a closed circuit. At this moment, the energy will be stored in the indicator. After the circuit is switched off, this energy will be evacuated. This is why the output voltage converter is stable and has greater value than the input voltage. Then, in the feedback, the voltage level is sensed and sent to the comparator to find the error value. The error signal is then sent to a PI controller for correcting the output voltage. The reason for using PI controller instead of PID is that if the derivative term (D) is added to the boost control system, the presence of high-frequency noise in the boost converter has been highly amplified. The derivative term can also be trouble maker during a sudden variation in the input reference such that If a big sudden variation happens, the mentioned momentary variation in the error e(t) that is multiplied by the derivative constant ($\mathrm{K_D}$) will saturate the converter.

The modulator is finally adopted to form the optimal PWM signal for igniting the MOSFET. In this study, the optimal value of the PI controller is obtained by the proposed optimization algorithm.

Table 2
The adopted values for the load distribution simulations of the BTS and the boost converter.

Load distribution parameters in the BTS	
Battery voltage	48 V
Number of BTS at the site	1
Total BTS load (Transceiver + microwave)	2380 W, 50 A
Heat exchanger load	360 W
Microwave equipment load	100 W
Load/Transceiver	12
Transceiver	160 W
Parameters of boost converter	
Inductance	0.01 mH
Input voltage	26–39 V
Output voltage	48 V
Resistance	1.2 Ω
Conductance	21.6 mF
f_s	10 kHz

In this study, the state-space model of the system has been utilized so that two states model is employed due to two active elements, i.e. the voltage of the capacitor and the current of the inductor.

$$\dot{x} = \begin{bmatrix}\alpha & \beta \\ \gamma & \delta\end{bmatrix} x + \begin{bmatrix}\rho \\ \sigma\end{bmatrix} V_{in} \quad (9)$$
$$y = \begin{bmatrix}\tau & \omega\end{bmatrix} x$$

By considering the switch into state "on",

$$\alpha = -\frac{r_L}{L}, \beta = \gamma = \sigma = \tau = 0, \delta = -\frac{1}{C\left(R + r_c\right)}, \rho = \frac{1}{L}, \omega = \frac{R}{R + r_c} \quad (10)$$

And, by considering the switch into state "off",

$$\alpha = \frac{r_L + \frac{Rr_C}{R+r_C}}{L}, \beta = -\gamma = -\frac{R}{C\left(R + r_c\right)}, \delta = -\frac{1}{C\left(R + r_c\right)}, \rho = \frac{1}{L}, \sigma = 0, \tau = \frac{Rr_C}{R + r_C}, \omega = \frac{R}{R + r_c} \quad (11)$$

A comprehensive model of the system is obtained by the averaged large-signal model within the circuit averaging when it is in "ON" state and "OFF" state of the switch over a cycle as:

$$\alpha = \frac{r_L}{L}D + \frac{r_L + \frac{Rr_C}{R+r_C}}{L}\left(1 - D\right), \beta = -\gamma = -\frac{R}{C\left(R + r_c\right)}\left(1 - D\right), \delta = -\frac{1}{C\left(R + r_c\right)}, \rho = \frac{1}{L}, \sigma = 0, \tau = \frac{Rr_C}{R + r_C}\left(1 - D\right), \omega = \frac{R}{R + r_c} \quad (12)$$

where, $\mathrm{DT_S}$ and $(1-D)\,T_S$ represent "ON" and "OFF" states of the switch.

Table 2 illustrates the adopted values for the load distribution simulations of the BTS and the boost converter.

The combination of the boost converter and the optimization algorithm forms the regulating unit. This unit adjusts the source and the load voltages by increasing the voltage level. Furthermore, the distribution DC bus for BTS requires a reliable, adjusted, and uninterrupted 48 V DC power source. This reliable

voltage can be provided by the boost converter by considering a low oscillation at the output. A significant case that should be considered in the system is to design a reliable system that can recovery itself after sudden disturbances with minimum time, overshoot, and undershoot. This forces us to use a closed-loop control system for this purpose.

5. Barn owl and inspiration for optimization

In recent years, the application of bio-inspired techniques is turned into popular global optimization methods. the main idea behind these techniques is to mimic different natural phenomena (Saeedi et al., 2019; Nejad et al., 2019; Mousavi and Soleymani, 2014), social behavior (Gheydi et al., 2016; Aliniya and Mirroshandel, 2019; Atashpaz-Gargari and Lucas, 2007; Razmjooy et al., 2011, 2013, 2017b), human competitions (Razmjooy et al., 2016; Bandaghiri et al., 2016; Razmjooy et al., 2017a, 2018), etc.

Intensification and diversification are important characteristics of the meta-heuristic methods. Intensification searches around the current best solutions and selects the best candidate points.

The convergence ability and escaping from the local optimum point are important parts of these techniques. Several new bio-inspired algorithms are proposed for global search. Recently, Jain et al. (2018) developed a promising bio-inspired technique, owl search algorithm (OSA). The OSA is based on the idealized behavior of the hunting characteristics of owls.

The owl is a bird that lives all over the globe except Antarctica. These birds hunt at night, which is why they are known as night predators. The owl is widely believed to be an infelicitous bird, but it is a useful hunter because it can be used to kill rodents. The eyes of owl are like a human being in front of his face. However, owls cannot move their eyes and have to turn their heads and neck to see their surroundings.

The owl is an elongated owl, with wide wings, bright color, and almost square tail. Depending on the subspecies, its length is 2 to 4 cm and its wing width is 1 to 2 cm. On the fly, they can be cleaned of ordinary owls by the movements of the waves and the legs covered with feathers.

Its back surface is golden pea-colored and has tiny spots and has a fairly uniform white ventral surface. Its eyes are black and he has no guppers. It usually hunts at night by sitting upright with their long legs and big head. The owl's face and legs are full of feathers. The male and female owls are similar, but the female owl has a larger size than the male. The species vary in size and can range from 15 cm to 76 cm.

The owl has very good hearing and vision. The owl's visual power is so high that it can help it hunting in the dark. Some owls also hunt with their high hearing power.

The barn owl is the most diverse species among different kinds of owls. Barn owls live in everywhere except poles and desserts from the alpine belt, large parts of Indonesia and the islands of the ocean. It is a beautiful hunter bird at night, with a medium-sized white and large feather, it has a short, square tail and long legs and its legs are covered with white feathers. They have a great auditory system for locating the prey. Barn owls have grown with a determined anatomical characteristic of auditory system by vertical asymmetry of ears. This specific characteristic is used to obtain the sound in one ear before the other to exact locating of prey (Grothe, 2018).

The prey can be hidden in the dark by hearing sense instead of vision sense (Moiseff et al., 2018). The generated sound by prey is processed based on twp parts in the owl's brain: the interaural level (loudness) difference (ILD) and the interaural time difference (ITD) which are used for preparing the auditory map of prey location (Jain et al., 2018). The owl can estimate the prey distance based on time and intensity differences of sound wave arrival.

5.1. Owl search algorithm (OSA)

Like any bio-inspired optimization algorithms, OSA starts with a random set of the population as the initial solution of the algorithm. The population in OSA shows the position of owls in a forest as the search space. By considering n number of owls and d dimensional search space, the random position for owls is stored in n × d matrix as follows:

$$O = \begin{bmatrix} O_{1,1} & \cdots & O_{1,d} \\ \vdots & \ddots & \vdots \\ O_{n,1} & \cdots & O_{n,d} \end{bmatrix} \tag{13}$$

where, matrix element $O_{i,j}$ describes the jth variable (dimension) of ith owl. To generate a uniform distributed initial location, the following formula has been applied:

$$O_i = O_l + (O_l + O_u) \times U(0, 1) \tag{14}$$

where, U (0, 1) represents a uniformly distributed random integer in the interval 0 and 1, and O_u and O_l upper and lower bounds of ith owl O_i in jth dimension, respectively.

The cost for the owls' location in a forest is calculated based on a cost function and stored in a matrix as follows:

$$f = \begin{bmatrix} f_1\left(\left[O_{1,1}, O_{1,2}, \ldots, O_{1,d}\right]\right) \\ \vdots \\ f_n\left(\left[O_{n,1}, O_{n,2}, \ldots, O_{n,d}\right]\right) \end{bmatrix} \tag{15}$$

The cost value of the owls' location here directly depends on the intensity information received through ears. In this condition, maximum intensity (for maximization problems) can be obtained by the best owl as it is more close to prey. The normalized intensity value information of ith owl is adopted for updating the position and may be achieved by:

$$I_i = \frac{f_i - w}{b - w} \tag{16}$$

where,

$$b = \max_{m \in 1,\ldots,n} f_m \tag{17}$$

and,

$$w = \min_{m \in 1,\ldots,n} f_m \tag{18}$$

The distance information for each owl and prey is formulated as follows:

$$D_i = \sqrt{\sum_i (O_i - L)^2} \tag{19}$$

where L represents the prey location that is obtained by the fittest owl.

The algorithm considers that there is only one prey (global optimum) in the forest. In the hunting process, owls flights silent towards the prey. The intensity changing for the ith owl is achieved below:

$$C_i = \frac{I_i}{{D_i}^2} + R_n \tag{20}$$

where, ${D_i}^2$ is used instead of $4\pi {D_i}^2$, and R_n is random noise to make the model more realistic.

Due to the prey movements, the owls need to change their present location silently. In OSA, the prey movement is modeled

based on probability and therefore new positions of owls are achieved by the following position updating mechanism:

$$O_i^{t+1} = \begin{cases} O_i^t + \beta \times C_i \times \left|\alpha L - O_i^t\right|, & p_{pm} < 0.5 \\ O_i^t - \beta \times C_i \times \left|\alpha L - O_i^t\right|, & p_{pm} \geq 0.5 \end{cases} \quad (21)$$

where, p_{pm} describes the probability of prey movement, α and β present a uniformly distributed random number in the range [0, 0.5] and a linearly decreasing constant from 1.9 to 0, respectively.

Indeed, β is a large variation that develops the exploration term of the search space. By developing these variations using the algorithm, it can be reduced to improve the exploitation. The OSA has only one parameter (β) that makes it so reliable than the other bio-inspired algorithms.

5.2. Improved balanced owl search algorithm (BOSA)

In recent years, by increasing the impact of nonlinear dynamics in system modeling, the application of chaos theory has been increasing. Optimization is one of the fields which can be impressed by the chaos theory.

From the standard OSA, the parameter β is the only random value in the algorithm. Using random values in each iteration makes a premature convergence for the system. In this study, to cover this problem, a chaos mechanism, called singer mapping has been employed (Yang et al., 2007; Rim et al., 2018). This mechanism maps the unknown parameter β into a regular formulation:

$$\beta_{i+1} = 1.07\left(7.9\beta_i - 23.3\beta_i^2 + 28.7\beta_i^3 - 13.3\beta_i^4\right) \quad (22)$$

Another technique for improving the premature convergence in OSA is to use Lévy flight (LF). LV is a popular mechanism that is widely used in bio-inspired optimization algorithms to develop premature convergence (Choi and Lee, 1998). The random walk is the main part of this mechanism for proper handling of the local search. This mechanism is mathematically formulated as follows:

$$Le(w) \approx w^{-1-\tau} \quad (23)$$

$$w = \frac{A}{|B|^{1/\tau}} \quad (24)$$

$$\sigma^2 = \left\{\frac{\Gamma(1+\tau)}{\tau\Gamma((1+\tau)/2)}\frac{\sin(\pi\tau/2)}{2^{(1+\tau)/2}}\right\}^{\frac{2}{\tau}} \quad (25)$$

where, τ describes the LV index in the range [0,2] (here, $\tau = 3/2$ Li et al., 2018), $A \sim N(0, \sigma^2)$ and $B \sim N(0, \sigma^2)$, w is the step size, $\Gamma(.)$ Determines Gamma function, $A/B \sim N(0, \sigma\ 2)$ means that the samples produce from a Gaussian distribution in which mean is zero and variance is σ^2, respectively.

Based on the explained cases, new positions of the owls can be achieved by the following formulation:

$$O_i^{t+1} = \begin{cases} O_i^t + \beta \times C_i \times \left|\alpha L - O_i^t\right| \times Le(\delta), & p_{pm} < 0.5 \\ O_i^t - \beta \times C_i \times \left|\alpha L - O_i^t\right| \times Le(\delta), & p_{pm} \geq 0.5 \end{cases} \quad (26)$$

The flowchart of the presented IOSA is shown in Fig. 3.

5.3. The validation of the algorithm

To validate the proposed algorithm, four standard benchmarks have been analyzed. The algorithm is compared with some new algorithms including emperor penguin optimization (EPO) (Dhiman and Kumar, 2018), shark smell optimization (SSO) algorithm (Abedinia et al., 2018), world cup optimization algorithm (WCO) (Razmjooy et al., 2016), and the original OSA.

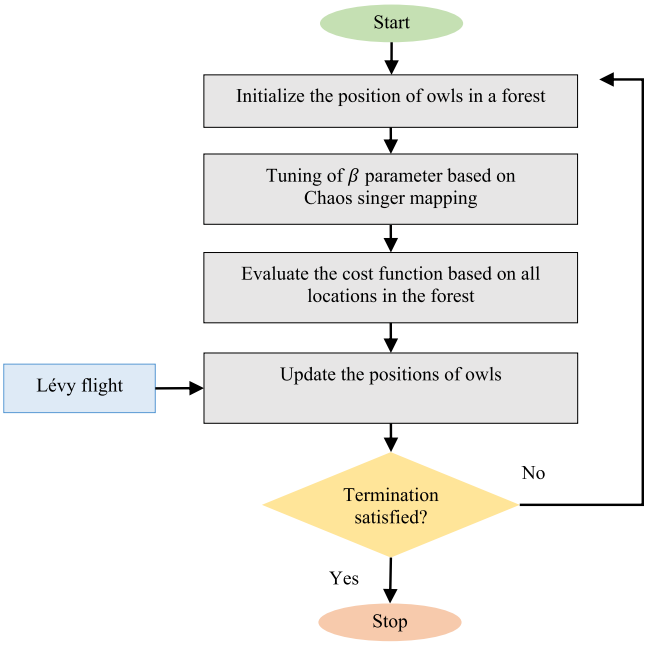

Fig. 3. Block diagram of the proposed BOSA.

The first benchmark is Rastrigin with a dimension between 30 and 50 and constraints in the range [−512, 512]:

$$f_1(x) = 10D + \sum_{i=1}^{D}\left(x_i^2 - 10cos(2\pi x_i)\right) \quad (27)$$

The second benchmark is Rosenbrock with a dimension between 30 and 50 and constraints in the range [−2.045, 2.045]:

$$f_2(x) = \sum_{i=1}^{D-1}\left(100\left(x_i^2 - x_{i+1}\right) + (x_i - 1)^2\right) \quad (28)$$

The third benchmark is Ackley. This benchmark has a dimension between 30 and 50 with the constraints in the range [−10, 10] which can be formulated as follows:

$$f_3(x) = -20exp\left(-0.2\sqrt{\frac{1}{D}\sum_{i=1}^{D}\left(x_i^2\right)}\right) - exp\left(\frac{1}{D}\sum_{i=1}^{D}(cos(2\pi x_i))\right) + 20 + e \quad (29)$$

And the last benchmark is Sphere. This benchmark has a dimension between 30 and 50 with the constraints in the range [−512, 512] which can be formulated as follows:

$$f_4(x) = \sum_{i=1}^{D} x_i^2 \quad (30)$$

Table 3 declares the simulation results of the presented method compared with others.

The results show that using the proposed method gives the best achievements compared with the other state of the art methods.

6. The main architecture of the optimized system for the telecom supply system

The main structure of the supply system includes a boost converter, a modulator, a comparator, and a controller. MOSFET

Table 3
The obtained results of the different algorithms for validation.

Benchmark		IOSA	EPO	GA (Nejad et al., 2019)	SSO (Bansal, 2019)	WCO (Razmjooy et al., 2016)	OSA
f_1	MD	0.00	2.28	70.61	74.24	2.19	3.15
	SD	0.00	3.53	1.66	8.96	4.35	3.74
f_2	MD	4.28	13.10	35.41	200.1	13.16	12.95
	SD	3.62	4.72	27.15	59.00	4.62	7.6
f_3	MD	0.00	6.32e−16	3.19e−2	8.26	3.14e−3	4.85e−16
	SD	0.00	0.00	2.14e−2	1.19	1.12e−3	0.00
f_4	MD	0.00	0.00	1.15e−4	8.27e−4	6.19e−9	0.00
	SD	0.00	0.00	3.14e−5	5.12e−4	3.28e−9	0.00

Table 4
Parameter setting of the algorithms.

Algorithm	Parameter	Value
PSO	No. of particles	100
	No. of generation	1000
	c_1 and c_2	2
	Inertia weight	0.9
EPO	Search agents	100
	No. of generation	1000
	Temperature profile	500
	$\vec{A}$ Constant	[−1.5, 1.5]
	Function S ()	[0,1.5]
	Parameter M	2
	Parameter f	2.5
	Parameter l	1.5
IOSA	Search agents	100
	No. of generation	1000

is used here for tuning the boost converter based on switching on and switching off.

As aforementioned, to proper control of the PEMFC in the base transceiver station, the feedback signal of the output voltage ($V_O(t)$) is sensed and compared with the desired voltage ($V_D(t)$) to detect the value of the error signal, i.e.

$$E(t) = V_D(t) - V_O(t) \tag{31}$$

Afterward, the op-amp receives the error signal to operate as PI controller. To achieve optimal coefficients (the proportional (K_P) and the integral (K_I) coefficients) for the controller, IOSA has been utilized, such that:

$$u(t) = K_p + K_I \int E(t) \tag{32}$$

The reason for selection the OSA was its results for global optimization in comparison with the other new introduced algorithms. This is also proved after applying its improved version to the Telecom system. It is important to note that this algorithm gives good results for our case study, in other words, it is not guaranteed to give the best results for other applications which shows the nature of the meta-heuristics. To present an impartial evaluation, common parameters of all the algorithms including the number of iteration (1000) and the population are considered to be the same. More setting are given in Table 4.

The standard parametric settings of algorithms are used as given in Table 2. A valid statistical analysis is performed by independently executing each algorithm for 30 trial runs for each benchmark function with maximum 30 000 number of function evaluations in each run. The recorded results are presented in Table 3 in terms of their best, worst, mean value and standard deviation (SD).

Then, the modulator applies an optimal PWM signal control for igniting the MOSFET. This process makes an optimal configuration for the boost converter in the DC distribution bus of the BTS. Fig. 4 shows the architecture of the boost converter by feedback method including a comparator, modulator, and PI controller.

Ziegler–Nichols (ZN) is a method that steps up the proportional coefficient so long as the feedback system becomes critically stable. However using ZN as a classic method for adjusting the controller coefficient is a good selection; it sometimes stuck in the local minimum. To solve this problem, as aforementioned in this study, a new optimization technique, called IOSA is proposed for achieving a global minimum value of the error signal for the boost converter. The method has also the ability to prevent premature convergence. The cost function for the converter optimization in this research is declared below:

$$\min F(K_P, K_I) = \frac{1}{t} \int_0^{\infty} t \times E(t)^2 dt \tag{33}$$

Subject to,

$$K_{P,min}, K_{I,min} \leq K_P, K_I \leq K_{P,max}, K_{I,max} \tag{34}$$

And the cost of the fitness function is:

$$Cost\ function = \frac{1}{1 + F(K_P, K_I)} \tag{35}$$

where, $\theta = f(K_P, K_I)$.

7. System analysis

As before mentioned, this study analyzes a new supply configuration in the presence of PEMFC for base transceiver station in a remote area. The proposed architecture has two main advantages. Firstly, using this system reduces the requirement for multiple batteries package. Secondly, this configuration provides green energy instead of diesel generator. The study utilized a new optimized configuration of the boost converter based on a new algorithm, called BOSA, to generate an interface between PEMFC and BTS load to achieve a regulator with quick dynamic response.

In this study, a 30 V, 1.8 kW PEMFC is considered in a standard condition. Nevertheless, changes in the load and environment such as temperature and humidity put the output voltage of the PEMFC in the range 26 V and 39 V. In addition, changes in the number of the transceivers make some variations on the power of the telecom load in the range 500 W and 2200 W. Therefore, the main purpose is to provide a regulator to achieve a stable voltage for the distribution bus of the BTS in 48 V by considering the aforesaid variations.

In this study, the efficiency of the presented optimized system based on IOSA for regulating the BTS supply is compared with the classical PI controller, i.e. ZN method and also the standard OSA and Emperor Penguin Optimizer (EPO) (Dhiman and Kumar, 2018) as one of the newly proposed optimization algorithm to have a fairy analysis. Three different scenarios have been validated for the system analysis as follows:

(1) Analysis of the tracking ability of the output voltage from the desired voltage (V_d) with ±10% variations for the voltage of the distribution bus, i.e. [43 V, 53 V].

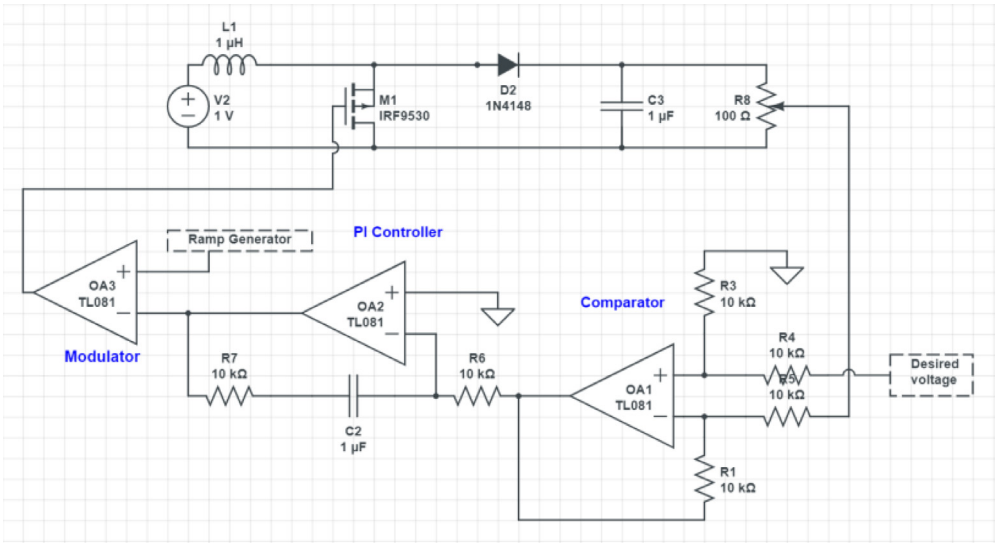

Fig. 4. The architecture of the boost converter by feedback method and PI controller.

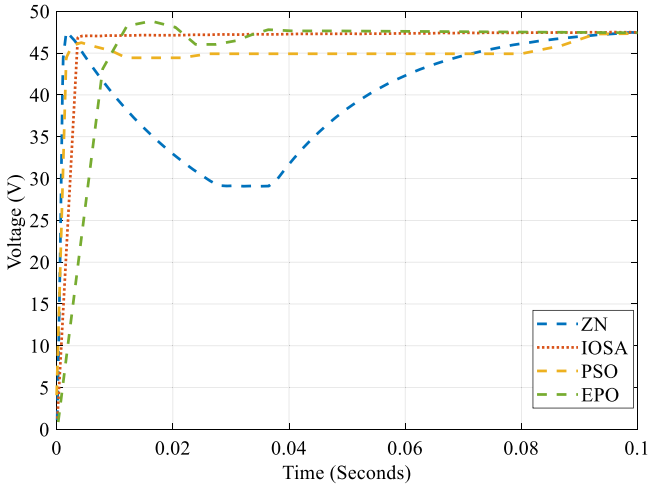

Fig. 5. The dynamic response of the proposed IOSA compared with the analyzed methods during an increasing input voltage from 0 to 30 V.

(2) Analysis of the disturbance rejection ability of the regulator by considering the input voltage (V_{in}) changes in the boost converter in the range [26 V, 39 V].
(3) Analysis of the disturbance rejection in the output by considering the controller efficiency for 22% of overloading and 72% of under loading condition when the peak traffic of the communication signals and when only a transceiver works, respectively.

Simulation results have been applied by the Matlab R2017b platform. In this part, the proposed method has been compared with ZN method as a classic controller and also PSO algorithm and EPO algorithm (Dhiman and Kumar, 2018) as optimized algorithms.

At first, consider a voltage step-up from 0 V to 30 V whereas the purpose is to track the desired voltage ($V_d = 49$ V) of 1.8 kW load. Fig. 5 shows the dynamic response of the proposed IOSA based system compared with the analyzed methods.

As can be seen, the proposed IOSA technique has the fastest results for the studied case study while the ZN method as a classic method has the worst results such that it has about 20% undershoot and it decreases to about 29.5 V at that time. This shows how the optimization algorithms can improve system efficiency.

Table 5
The regulator PI parameters achieved by different methods.

Fitness function	Algorithm	K_P	K_I
MSE	ZN	0.0406	8.12
	BOSA	6.3	62.81
	EPO	5.7	71.4
	PSO	1.6	88.3

Table 6
A detailed study on the system dynamic response.

Dynamic response characteristic	ZN	IOSA	EPO	PSO
Settling time (ms)	96.37	10	35	84
Rise time (ms)	1.2	1.1	1.2	0.3
Overshoot (%)	–	–	20	–
Peak time (ms)	4	5	18	2

It can be also observed that the results of the proposed IOSA regulator have no undershoot or overshoots in this condition. Settling time for this method is about 5 ms. Table 5 illustrates the PI parameters that are achieved by the proposed method and the ZN, PSO, and EPO methods and Table 6 declares the system dynamic response based on these values.

In Fig. 6, we consider an input voltage step up from 26 V to 39 V at time 0.5 s. The settling time of the introduced IOSA-based regulator is about 48.82 ms by an overshoot of less than 5%. Here, using ZN based regulator, PSO based regulator, and EPO based regulator gives 51.4 s, 49.4 s, and 49.9 s, respectively.

In the following, a reverse state has been considered. By assuming a drop down for the input voltage from 39 V to 26 V at time = 0.5 s, the settling time for the introduced BOSA, ZN, PSO, and EPO based regulators are 42.54 ms, 60.5 ms, 53 ms, and 44.6 ms, respectively. In addition, the output of the proposed IOSA is the closest results to the desired voltage during the input perturbation (see Fig. 7).

In Fig. 8, the load oscillation for the studied system in about 4.6 Ω has been shown.

The results of this variation are shown in Fig. 9. It can be seen that the dynamic response of the boost converter by ZN regulator

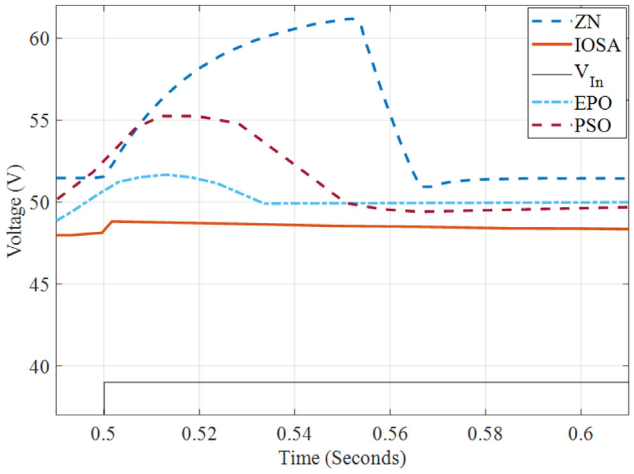

Fig. 6. The dynamic response of the proposed IOSA compared with the analyzed methods during an increasing input voltage from 0 to 30 V.

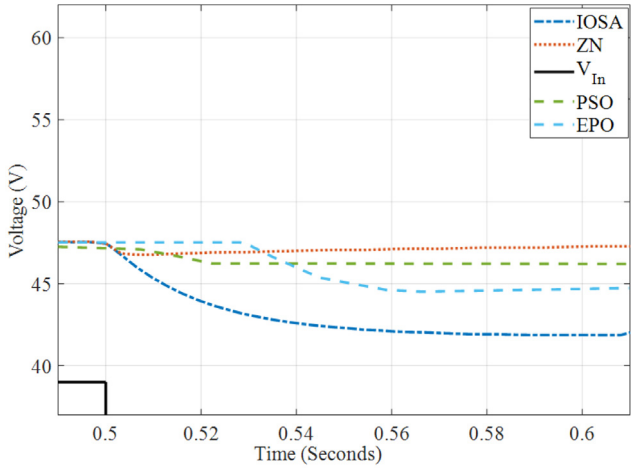

Fig. 7. The dynamic response of the proposed IOSA compared with the analyzed methods during an increasing input voltage from 30 to 0 V.

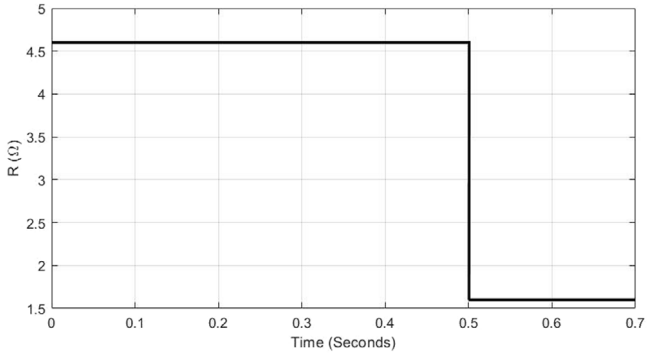

Fig. 8. The load variations for the studied system in about 4.6 Ω.

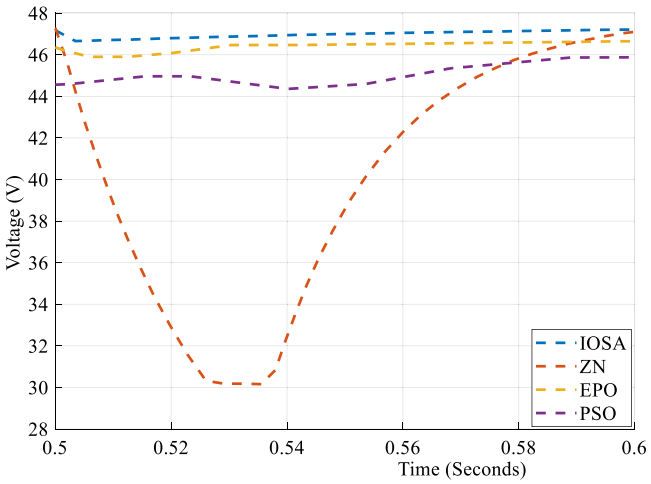

Fig. 9. The output voltage of the system by the proposed IOSA compared with the analyzed methods for optimizing boost converter for the load variation at time 0.5 s.

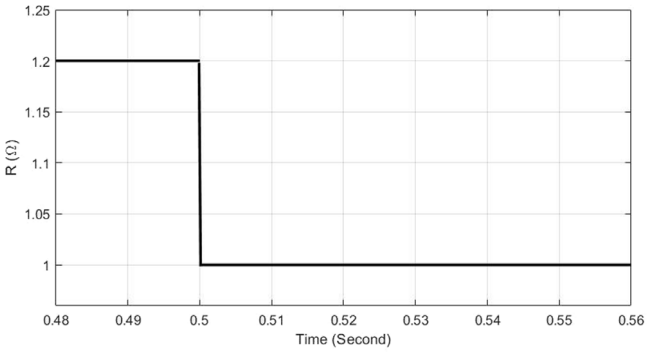

Fig. 10. The load variations for the studied system in about 1.2 Ω.

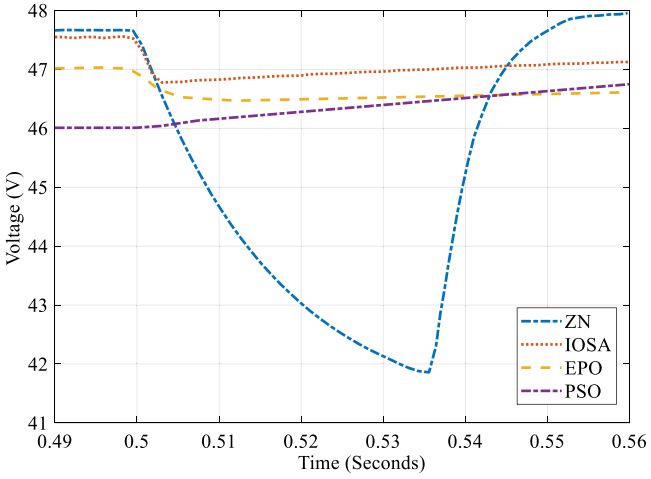

Fig. 11. The output voltage of the proposed IOSA compared with the analyzed methods for load variation at time 0.5 s.

indicates an extra undershoot to the 28.7 V at the time 30.2 ms. Other methods have good results for this case.

In Fig. 10, the load oscillation for the studied system in about 1.2 Ω has been shown and the results are shown in Fig. 11.

As can be seen, the settling time for the proposed IOSA, ZN, EPO, and PSO is achieved 56 ms, 56 ms, 56 ms, and 46.61 ms, respectively. The output of the proposed method gives the best results compare with the other methods.

Consider another condition with a value of ±10% oscillations from the desired voltage which is applied at the time 0.5 s. Figs. 12 and 13 show 53 V and 48 V load variation at time 0.5 s, respectively. It is observed that among different methods, the

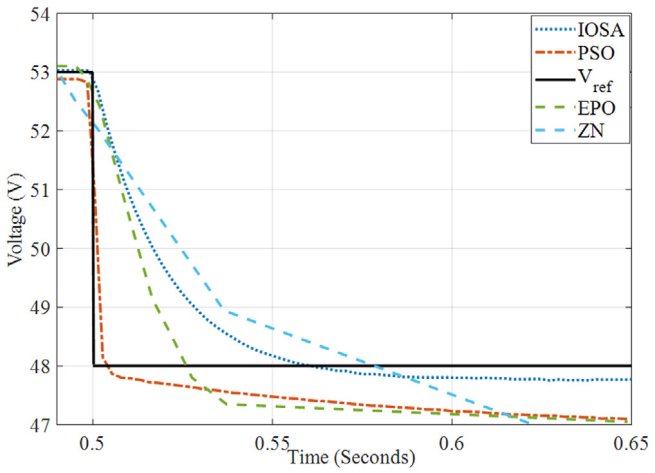

Fig. 12. Step response for ±10% oscillations of the output voltage in the proposed IOSA compared with the analyzed methods.

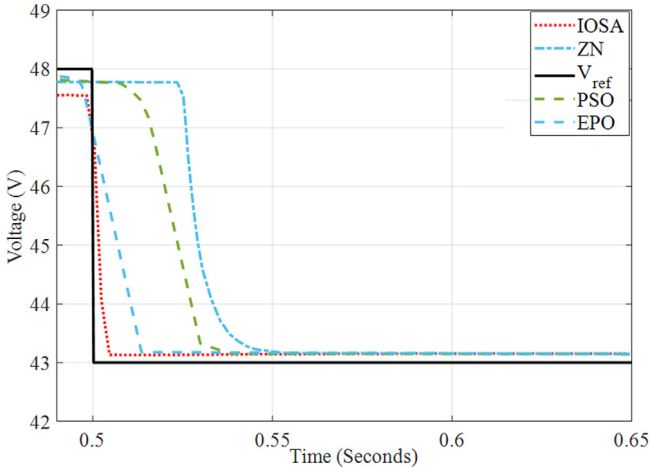

Fig. 13. Step response for ±10% oscillations of the output voltage in the proposed IOSA compared with the analyzed methods.

ZN based regulator has the most delay for the dynamic response while the proposed IOSA has the best results.

8. Conclusion

This study presents a new optimized method for PEMFC based energy conversion system to supply guaranteed energy for a telecom system. The main objective is to develop the system efficiency to decrease the operating cost. By considering the PEMFC along with DC distribution bus with output voltage regulation, the reliability and the power supply quality have been increased and make it interruptible to the loads. The regulator is designed based on the PI technique to hold the output voltage of the boost converter in the 48 V. A new improved version of the Owl search algorithm based on Singer mapping and Levy flight is proposed to improve the PI controller. For the performance analysis of the proposed method, it has been compared with a classical method, Ziegler–Nichols based controller and some optimization based techniques including particle swarm optimization and emperor penguin optimizer based PI controllers to show the system performance that shows the excellence of the proposed method as an optimal regulator in the base transceiver station. In the future work, a combined cooling, heating, and power system along with Telecom tower will be proposed to improve the system efficiency.

Declaration of competing interest

The authors declare that they have no known competing financial interests or personal relationships that could have appeared to influence the work reported in this paper.

CRediT authorship contribution statement

Daming Li: Conceptualization, Data curation, Writing - original draft, Writing - review & editing. **Lianbing Deng:** Conceptualization, Data curation, Writing - original draft, Writing - review & editing. **Qinglang Su:** Conceptualization, Data curation, Writing - original draft, Writing - review & editing. **Yonghua Song:** Conceptualization, Data curation, Writing - original draft, Writing - review & editing.

Acknowledgments

1. Project funded by China Postdoctoral Science Foundation.
2. Project funded by National Key R&D Program of China (No. 2017YFB0503604 ; No. 2017YFB0503801).
3. Project funded by Electronic fence system project, China.
4. Project funded by the Project (0172018A) of FDCT, China.
5. Project funded by the Project of Macao Foundation, China.

References

Abedinia, O., Amjady, N., Ghadimi, N., 2018. Solar energy forecasting based on hybrid neural network and improved metaheuristic algorithm. Comput. Intell. 34, 241–260.
Aghajani, Gholamreza, Ghadimi, Noradin, 2018. Multi-objective energy management in a micro-grid. Energy Rep. 4, 218–225.
Akbary, Paria, et al., 2019. Extracting appropriate nodal marginal prices for all types of committed reserve. Comput. Econ. 53 (1), 1–26.
Aliniya, Z., Mirroshandel, S.A., 2019. A novel combinatorial merge-split approach for automatic clustering using imperialist competitive algorithm. Expert Syst. Appl. 117, 243–266.
Atashpaz-Gargari, E., Lucas, C., 2007. Imperialist competitive algorithm: an algorithm for optimization inspired by imperialistic competition. In: Evolutionary Computation, 2007. CEC 2007. IEEE Congress on. pp. 4661–4667.
Bagal, Hamid Asadi, et al., 2018. Risk-assessment of photovoltaic-wind-battery-grid based large industrial consumer using information gap decision theory. Sol. Energy 169, 343–352.
Bandaghiri, P.S., Moradi, N., Tehrani, S.S., 2016. Optimal tuning of PID controller parameters for speed control of DC motor based on world cup optimization algorithm. Parameters 1, 2.
Bansal, J.C., 2019. Particle swarm optimization. In: Evolutionary and Swarm Intelligence Algorithms. ed: Springer, pp. 11–23.
Choi, C., Lee, J.-J., 1998. Chaotic local search algorithm. Artif. Life Robot. 2, 41–47.
Choi, Y.B., Lee, J., Yoo, S., Yoo, Y.K., 2019. Value relevance of customer equity beyond financial statements: evidence from mobile telecom industry. Asia-Pac. J. Account. Econ. 26, 281–300.
Dhiman, G., Kumar, V., 2018. Emperor penguin optimizer: A bio-inspired algorithm for engineering problems. Knowl.-Based Syst. 159, 20–50.
Ebrahimian, Homayoun, et al., 2018. The price prediction for the energy market based on a new method. Econ. Res.-Ekon. Istraž. 31 (1), 313–337.
Eslami, Mahdiyeh, et al., 2019. A new formulation to reduce the number of variables and constraints to expedite SCUC in bulky power systems. Proc. Natl. Acad. Sci. India A 89 (2), 311–321.
Firouz, Mansour Hosseini, Ghadimi, Noradin, 2016. Concordant controllers based on FACTS and FPSS for solving wide-area in multi-machine power system. J. Intell. Fuzzy Systems 30 (2), 845–859.
Gheydi, Milad, Nouri, Alireza, Ghadimi, Noradin, 2016. Planning in microgrids with conservation of voltage reduction. IEEE Syst. J. 12 (3), 2782–2790.
Gollou, Abbas Rahimi, Ghadimi, Noradin, 2017. A new feature selection and hybrid forecast engine for day-ahead price forecasting of electricity markets. J. Intell. Fuzzy Systems 32 (6), 4031–4045.
Grothe, B., 2018. How the barn owl computes auditory space. Trends Neurosci. 41, 115–117.
Hallur, G.G., Sane, V.S., 2018. Indian telecom regulatory framework in comparison with five countries: structure, role description and funding, digital policy. Regul. Gov. 20, 62–77.
Hamian, Melika, et al., 2018. A framework to expedite joint energy-reserve payment cost minimization using a custom-designed method based on mixed integer genetic algorithm. Eng. Appl. Artif. Intell. 72, 203–212.

Hosseini Firouz, Mansour, Ghadimi, Noradin, 2016. Optimal preventive maintenance policy for electric power distribution systems based on the fuzzy AHP methods. Complexity 21 (6), 70–88.

Jain, M., Maurya, S., Rani, A., Singh, V., 2018. Owl search algorithm: a novel nature-inspired heuristic paradigm for global optimization. J. Intell. Fuzzy Systems 34, 1573–1582.

Kaur, R., Krishnasamy, V., Muthusamy, K., Chinnamuthan, P., 2017. A novel proton exchange membrane fuel cell based power conversion system for telecom supply with genetic algorithm assisted intelligent interfacing converter. Energy Convers. Manag. 136, 173–183.

Khodaei, Hossein, et al., 2018. Fuzzy-based heat and power hub models for cost-emission operation of an industrial consumer using compromise programming. Appl. Therm. Eng. 137, 395–405.

Leng, Hua, et al., 2018. A new wind power prediction method based on ridgelet transforms, hybrid feature selection and closed-loop forecasting. Adv. Eng. Inform. 36, 20–30.

Li, X., Niu, P., Liu, J., 2018. Combustion optimization of a boiler based on the chaos and Levy flight vortex search algorithm. Appl. Math. Model. 58, 3–18.

Liu, Yang, Wang, Wei, Ghadimi, Noradin, 2017. Electricity load forecasting by an improved forecast engine for building level consumers. Energy 139, 18–30.

Mahajan, V., Mahajan, R., Misra, R., 2019. Indian telecom industry: Challenges and use of analytics to manage customer churn. In: Handbook of Research on Expanding Business Opportunities with Information Systems and Analytics. ed: IGI Global, pp. 353–376.

Mirzapour, Farzaneh, et al., 2019. A new prediction model of battery and wind-solar output in hybrid power system. J. Ambient Intell. Humaniz. Comput. 10 (1), 77–87.

Moiseff, A., Haresign, T., Wang, J., 2018. Sound localization from binaural cues by the barn owl auditory system. In: Neuroethological Studies of Cognitive and Perceptual Processes. ed: Routledge, pp. 305–323.

Mousavi, B.S., Soleymani, F., 2014. Semantic image classification by genetic algorithm using optimised fuzzy system based on Zernike moments. Signal Image Video Process. 8, 831–842.

Nejad, Hadi Chahkandi, et al., 2019. Reliability based optimal allocation of distributed generations in transmission systems under demand response program. Electr. Power Syst. Res. 176, 105952.

Ojo, J.S., Owolawi, P.A., Atoye, A.M., 2019. Designing a green power delivery system for base transceiver stations in southwestern Nigeria. SAIEE Afr. Res. J. 110, 19–25.

Paudel, P., Wasti, S., 2018. Peak demand management in micro hydro using battery bank. Hydro Nepal: J. Water Energy Environ. 22, 34–40.

Razmjooy, N., Khalilpour, M., Ramezani, M., 2016. A new meta-heuristic optimization algorithm inspired by FIFA world cup competitions: Theory and its application in PID designing for AVR system. J. Control Autom. Electr. Syst. 27, 419–440.

Razmjooy, N., Madadi, A., Ramezani, M., 2017a. Robust control of power system stabilizer using world cup optimization algorithm. Int. J. Inform. Secur. Syst. Manag. 5, 7.

Razmjooy, N., Mousavi, B.S., Sadeghi, B., Khalilpour, M., 2011. Image thresholding optimization based on imperialist competitive algorithm. In: 3rd Iranian Conference on Electrical and Electronics Engineering (ICEEE2011).

Razmjooy, N., Mousavi, B.S., Soleymani, F., 2013. A hybrid neural network imperialist competitive algorithm for skin color segmentation. Math. Comput. Modelling 57, 848–856.

Razmjooy, N., Ramezani, M., Ghadimi, N., 2017b. Imperialist competitive algorithm-based optimization of neuro-fuzzy system parameters for automatic red-eye removal. Int. J. Fuzzy Syst. 19, 1144–1156.

Razmjooy, N., Sheykhahmad, F.R., Ghadimi, N., 2018. A hybrid neural network–world cup optimization algorithm for melanoma detection. Open Med. 13, 9–16.

Rim, C., Piao, S., Li, G., Pak, U., 2018. A niching chaos optimization algorithm for multimodal optimization. Soft Comput. 22, 621–633.

Saeedi, Mohammadhossein, et al., 2019. Robust optimization based optimal chiller loading under cooling demand uncertainty. Appl. Therm. Eng. 148, 1081–1091.

Yang, D., Li, G., Cheng, G., 2007. On the efficiency of chaos optimization algorithms for global optimization. Chaos Solitons Fractals 34, 1366–1375.